DEPARTMENT OF THE INTERIOR
U.S. GEOLOGICAL SURVEY

Isotopic evidence for evolution of sub-continental mantle during Red Sea rifting

by

John S. Pallister 1/ and Ernst Hegner

Open-File Report 89-335

Report prepared by the U.S. Geological Survey in cooperation with the Deputy Ministry for Mineral Resources, Saudi Arabia

1/ U.S. Geological Survey, Denver, CO

1989

TABLE OF CONTENTS

PAGE

ABSTRACT 1

INTRODUCTION AND OVERVIEW 2

GEOLOGY 2

DATA 4

CRUSTAL CONTAMINATION 9

CRUSTAL CONTAMINATION OR DUPAL MANTLE SOURCES? 13

MANTLE SOURCES FOR AL LITH MAGMAS 15
    Isotopic compositions 15
    Trace elements 16

MAGMA GENERATION AND MANTLE EVOLUTION 18

ACKNOWLEDGMENTS 20

DATA STORAGE 20

REFERENCES CITED 20

ILLUSTRATIONS

Figure

1. Simplified geologic map of the Al Lith quadrangle... 3

2. Comparison of extended LREE distribution paterns in enriched Al Lith basalts, plume-type mid-ocean ridge basalts (P-MORB) and ocean island basalts (OIB), and LREE-enriched island arc basalts (IAB)... 8

3. $^{87}Sr/^{86}Sr$ vs. $^{143}Nd/^{144}Nd$ isotopic compositions in Al Lith volcanics 8

4. Pb isotopic compositions in Al Lith rocks..... 10

PAGE

Figure

5. Variations of Pb/Sr with $^{87}Sr/^{86}Sr$, ϵ-Nd and $^{232}Th/^{238}U$ in Al Lith rocks plotted..... 11

6. $^{206}Pb/^{204}Pb$ ratios versus ϵNd values in Al Lith rocks..... 12

7. Diagrammatic model of mantle source evolution during Red Sea rifting..... 19

TABLES

Table

1. Pb, Sr, and Nd isotopic compositions in rocks from the Al Lith region..... 5

ISOTOPIC EVIDENCE FOR EVOLUTION OF SUB-CONTINENTAL MANTLE DURING RED SEA RIFTING

By

John S. Pallister and Ernst Hegner

ABSTRACT

Tertiary igneous rocks from near Al Lith, Saudi Arabia are alkaline to subalkaline and bimodal in composition, and document early and late rift volcanism (≥30 Ma to ≈20 Ma, 11 Ma and 3 Ma) in the central part of the Red Sea rift. Isotopic and trace-element data from twenty-five samples are presented and used to characterize basalt sources in the early rift.

Inferred primary isotopic compositions of alkalic basalts and some tholeiites indicate a common mantle source. Many of the felsic volcanics are isotopically indistinguishable from these mafic rocks; they likely represent products of fractional crystallization, or anatectic melts of mafic Al Lith precursors. $^{143}Nd/^{144}Nd$ and $^{87}Sr/^{86}Sr$ ratios for most Al Lith rocks show limited variation ($^{87}Sr/^{86}Sr_i = 0.7030$ to 0.7033, ϵ-Nd = +6 to +8). They plot near enriched MORB and between the isotopic compositions of recent magmas from the Red Sea spreading axis and less depleted to enriched basalts from the East African rift. Pb isotopic compositions are MORB-like and moderately radiogenic in $^{206}Pb/^{204}Pb$. Normalized imcompatible trace-element abundances and oceanic Pb/Ce indicate sources similar to those for enriched MORB and OIB and distinct from subduction-dominated source regions. As in many continental basalt fields, high $^{143}Nd/^{144}Nd$ and relatively low Sr and Pb isotopic ratios, despite incompatible-element enrichment, indicate that source enrichment was not an ancient event; it probably took place as a precursor to rift magmatism.

These data are consistent with a multi-stage model of sub-rift mantle evolution. Depleted lithospheric mantle in the spinel-lherzolite facies was veined by incompatible-element rich fluids, then partially melted. Melt equilibration and fractionation took place over a large depth range, producing transitional alkaline-subalkaline basalts during early rift magmatism. In the axis of the rift, depleted asthenospheric mantle upwelled and displaced the veined lithosphere, eventually producing MORB at the Red Sea axis. However, basalts from the veined lithospheric mantle continue to be erupted from the Arabian margin of the rift.

Anomalous, old (>2 Ga) continental-affinity Pb, radiogenic Sr and low ϵ-Nd values found in some of the subalkaline Al Lith rocks are explained by crustal contamination, not by Dupal mantle sources.

INTRODUCTION AND OVERVIEW

On the basis of xenolith studies, Menzies (1983) suggested a generalized model for the continental mantle and for continental alkaline magmatism. This model calls for depleted (oceanic type) layered upper mantle below continents that becomes locally enriched with incompatible elements by fluids and melts during kimberlitic-carbonatite and basanitic magmatism. Tertiary volcanic rocks from the Red Sea region and their entrained xenoliths provide a geochemical and petrologic "window" through which to view the conversion of sub-continental to sub-oceanic mantle. Because of this conversion, data from these rocks and from the exposed crust-mantle interface at Zarbagad Island, in the northern Red Sea (Bonatti others, 1981, 1986; Brueckner and others, 1987) provide important tests and constraints for sub-continental mantle models.

In this paper, we report Pb, Sr, and Nd isotopic compositions and mother/daughter-element concentrations for a suite of samples from the Red Sea coastal plain near the village of Al Lith (fig. 1). These igneous rocks were produced mainly during the early stages of Red Sea rift formation (>30 to ≈ 20 Ma). We also analyzed samples that were erupted in the same area during late stages of rift and paar development (11 and 3 Ma). On the basis of petrologic, geochemical, and preliminary Sr-isotopic data, Pallister (1987) proposed that compositional trends within the Al Lith suite are explained by polybaric mantle melting and reaction at depths of < 70 km.

Our results show that early rift volcanism at Al Lith was generated from moderately depleted sources that were isotopically intermediate between enriched mantle sources (East-African rift basalts, for example, Bell and Blenkinsop, 1987, continental basalts from the southern Arabian Shield, Menzies and Murthy, 1980) and oceanic-type asthenospheric mantle sources found in the Red Sea axis and Gulf of Aden (Betton and Civetta, 1984; Petrini, 1987; Cohen and others, 1980). A source-evolution model, in which ascending depleted asthenospheric mantle mixed with, and eventually displaced, locally-enriched lithospheric mantle, best explains the trace-element and isotopic-source signatures in the igneous rocks from the region. Our data is generally consistent with a pre- or early-rift sub-continental mantle model similar to that proposed by Menzies (1983). Our LREE-enriched basalts have high $^{143}Nd/^{144}Nd$ and most have non-radiogenic Sr and Pb ratios, consistent with element enrichment of source regions by fluids fractionated from underlying (and also depleted) mantle sources as an early phase of rift evolution.

GEOLOGY

The Al Lith area is characterized by widespread Late Proterozoic plutonic, metavolcanic and metasedimentary rocks of oceanic-arc affinity that are intruded and overlain by Tertiary volcanic, plutonic, and sedimentary rocks produced during Red Sea rifting. Most of the magmatic Tertiary rocks analyzed in this study belong

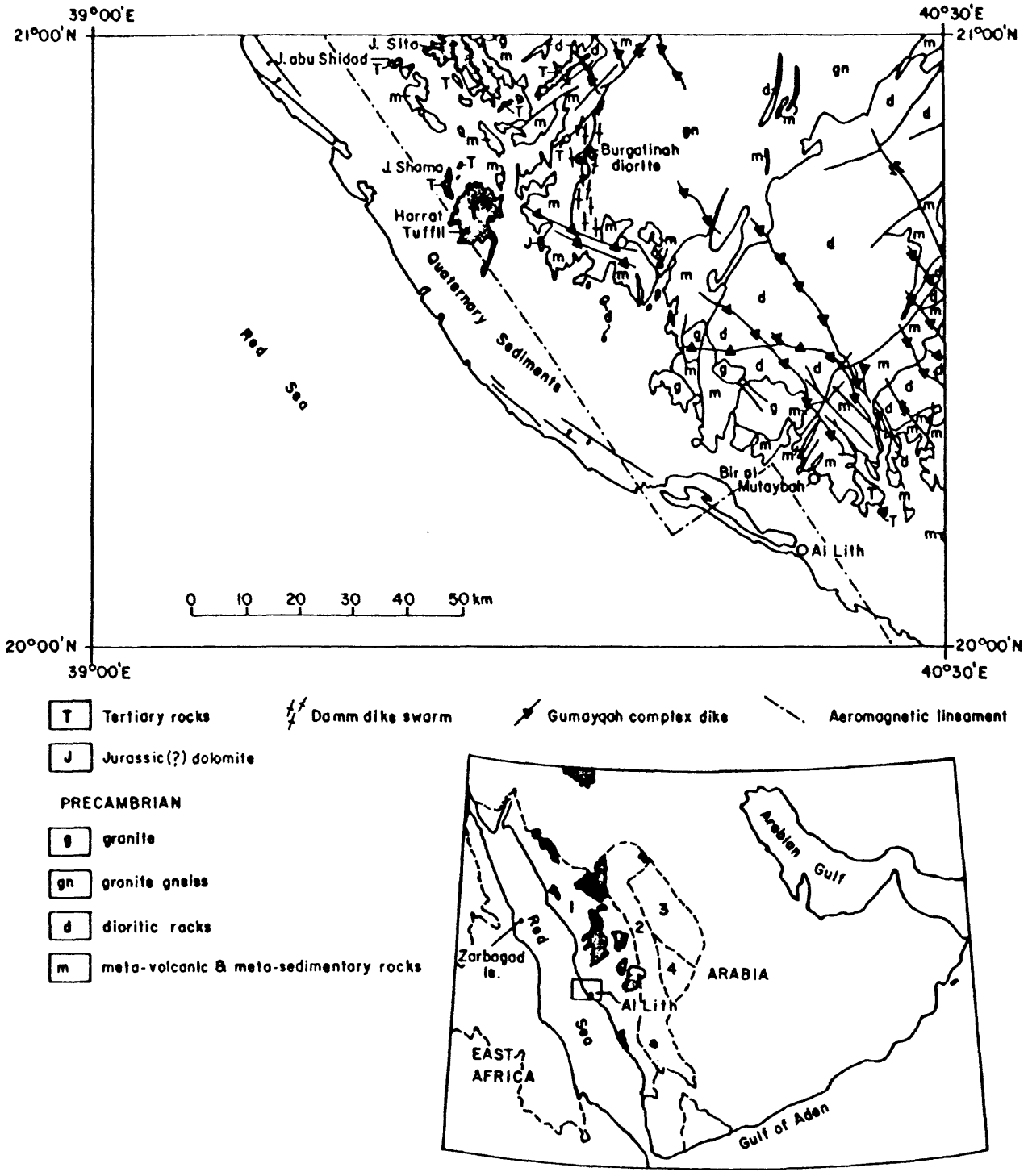

Figure 1.–Simplified geologic map of the Al Lith quadrangle (from Pallister, 1987) and index map of the Red Sea region showing location of the quadrangle. Index map also shows boundary of the Pan-African (Late Proterozoic) Arabian-Nubian Shield (ANS) and crustal provinces within the Arabian segment of the Shield (dashed lines) based on Pb-isotopic data from Stacey and Stoeser (1983): 1 = western arc terranes (oceanic), 2 = Nabitah mobile belt (oceanic), 3 = Afif terrane (oceanic), 4 = ancient gneiss terrane (continental). Harrat flood basalts are shown as stippled areas within index map. Volcanic and hypabyssal rock samples for this study from stippled (Tertiary) units shown on Al Lith quadrangle.

to the Sita formation and the Damm and Gumayqah intrusive complexes of Pallister (1987). These rocks occur in transitional continental-oceanic crust at the western (rifted) margin of the Arabian Shield (fig. 1).

The Sita formation is composed of bimodal mafic to felsic volcanics and is considered to be comagmatic with the Damm complex, which forms two prominent dike swarms. Intrusive relationships and K-Ar dating indicate a wide range in ages from >30 to ~20 Ma and peak of magmatism at about 30 Ma (Pallister, 1987). The Gumayqah complex (~20 Ma) intrudes the other assemblages and is preserved as widely-spaced, thick (to 100 m), gabbroic dikes.

Miocene (11 Ma) and Pliocene (3 Ma) alkali basalts and hawaiites occur in the Al Lith area as minor lava flows and as a small shield volcano. These rocks are part of the ~90,000 km^2 Harrat flood basalt province that was erupted through the western margin of the Arabian Shield during Red Sea rift and paar development (30 Ma to the present; Coleman and others, 1983).

DATA

Sr, Nd and Pb isotopic compositions and parent/daughter element concentrations for twenty-five mafic and felsic volcanic and dike samples are presented in table 1. Data for six gneisses and schists from Late Proterozoic basement rocks in the area are included and are used to evaluate magma contamination. Initial isotopic compositions were calculated assuming ages of 30 Ma for Sita volcanics and Damm dikes, 20 Ma for Gumayqah dikes and 10 Ma and 3 Ma for Miocene and Pliocene volcanics. Major-element concentrations and rare-earth element concentrations for selected samples were presented by Pallister (1987).

Extended light-rare earth element (LREE) distribution patterns for ten mafic rocks are schematically shown in figure 2. The sequence of element incompatibility and the patterns for average ocean-island basalts (OIB) and plume-type (P-type) MORB are from Sun (1980). The basalts are LREE-enriched, with element distribution patterns that are sub-parallel to average P-type MORB and OIB. Not seen are positive Pb, K and Sr anomalies typical of island-arc basalts (IAB) produced from sources affected by subduction processes. $^{147}Sm/^{144}Nd$ isotopic ratios (Table 1) for three basalts (165634, 165881, 175834) are close to the chondritic ratio of 0.1967, indicating unfractionated REE abundances in a few Al Lith basalts, although, the remaining $^{147}Sm/^{144}Nd$ data, as well as more complete INAA analyses (Pallister, 1987) show that most Al Lith basalts are LREE-enriched.

Nd and Sr isotopic compositions of most samples are similar to enriched MORB (fig. 3) or OIB. These samples show moderate variation in $^{143}Nd/^{144}Nd$ ratios, equivalent to ϵ-Nd values of +4 to +7.7 and $^{87}Sr/^{86}Sr$ isotopic compositions ranging from 0.7030 to 0.7035. Data for mafic, felsic, alkalic, and tholeiitic samples are overlapping, indicating common sources. Isotopic compositions of the late

Miocene alkali basalt and Pliocene hawaiite ("Harrat" basalts) are similar to the Eocene to early Miocene Al Lith rocks. Sr isotopic compositions in a few samples (with high Rb/Sr) plot to the left and right of the bulk of analyses. This is probably due to alteration of primary Rb and Sr concentrations, and (for high Rb/Sr samples) calculation of erroneous initial ratios because of imprecise age constraints, or in the case of several high $^{87}Sr/^{86}Sr$ ratios, to crustal contamination (as explained in the section that follows).

Table 1.--Pb, Sr, and Nd isotopic compositions in rocks from the Al Lith region.

Pb-isotopic data corrected for 0.14% mass fractionation per a.m.u., $^{143}Nd/^{144}Nd$ ratios normalized to $^{146}Nd/^{144}Nd$ = 0.7219. ENd based on $^{143}Nd/^{144}Nd$ = 0.512638 for present day CHUR and calculated using the method of DePaolo and Wasserburg (1976). $^{143}Nd/^{144}Nd$ ratios are relative to 0.511865 (La Jolla Nd standard); $^{87}Sr/^{86}Sr$ ratios are relative to 0.71026 (NBS-SRM987 standard). Delta-8/4 values calculated using the method of Hart (1984). Blanks (in ng): Pb = 0.10-0.15, U < 0.01, Th < 0.01, Rb = 0.0-0.1, Sr = 0.5-1.0, Sm < 0.1, Nd < 0.1. Rb determined by XRF, other elements by isotope dilution. Initial (i) isotopic ratios calculated assumming 30 Ma for Damm complex and Sita Formation, 20 Ma for Gumayqah complex, 10 Ma for Harrat lava 165666, and 3 Ma for Harrat lava 165006. Additional radiometric, geochemical, petrographic, and geologic data for samples given in Pallister (1987) and references therein.

	Harrat lavas		Gumayqah complex dikes			Damm complex dikes		
Sample No.	165006	165666	165634	175764	175776	165574	165546	165559
Rock type	Hawaiite	A.basalt	Gabbro (A.basalt)	Gabbro (basalt)	Diabase (basalt)	Qz.dior. (dacite)	Rhyolite	Hawaiite
N. Latitude	20°43.6'	20°59.2'	20°53.3'	20°28.0'	19°23'	20°47.7'	20°44.3'	20°49.0'
E. Longitude	39°41.5'	39°39.1'	39°56.5'	40°12.2'	41°15'	39°51.3'	39°53.4'	39°51.9'
$^{206}Pb/^{204}Pb$	18.86	18.99	18.16	18.42	18.44	18.05	18.24	18.18
$^{206}Pb/^{204}Pb(i)$	18.85	18.94	18.14	18.39	18.41	18.02	18.19	18.16
$^{207}Pb/^{204}Pb$	15.55	15.56	15.55	15.57	15.58	15.51	15.54	15.51
$^{208}Pb/^{204}Pb$	38.58	38.72	37.92	38.68	38.56	37.74	37.83	37.77
$^{87}Sr/^{86}Sr$	.70313±3	.70309±2	.70329±3	.70451±2	.70426±2	.70324±2	.74247±3	.70354±2
$^{87}Sr/^{86}Sr(i)$	.70302	.70308	.70324	.70449	.70424	.70318	.70506	.70338
$^{143}Nd/^{144}Nd$	.51293±1	.51295±1	.51293±2	.51228±2	.51229±2	.51288±2	.51285	.51303±1
ENd	5.6	6.2	5.7	4.8	5.5	5.0	4.3	7.7
U	1.09	.78	0.05	0.38	.36	0.78	0.27	0.14
Th	3.31	2.26	0.18	2.12	1.34	2.83	31.02	0.51
Pb	2.39	1.55	0.51	2.67	2.12	7.97	55.13	2.12
$^{238}U/^{204}Pb$	29.1	32.5	6.0	9.1	11.0	6.1	11.7	4.2
$^{232}Th/^{238}U$	3.1	3.0	3.7	5.7	3.8	3.7	3.1	3.7
Rb	20	20	10	10	<10	20	290	45
Sr	711	606	176	414	294	415	9.6	348
Nd	32.58	29.13	4.33	34.97	21.77	34.53	25.47	18.21
Sm	6.64	6.04	1.41	8.15	5.33	7.78	6.76	4.79
$^{147}Sm/^{144}Nd$	.123	.125	.197	.141	.148	.136	.169	.156
$Pb/SrX10^3$	3.3	2.6	2.9	6.4	7.2			6.1
delta-8/4	17	21						19

Table 1.--Pb, Sr, and Nd isotopic compositions (continued)

	Damm complex dikes							
Sample No.	165571	165572	165627	165661	165881	165882	175780	175834
Rock type	Basalt	Dacite	Comendite	Diabase (Hawaiite)	Basalt	Hawaiite	Diabase (Basalt)	Basalt
N. Latitude	20°47.7'	20°47.7'	20°48.6'	20°56.8'	20°52.4'	20°54.2'	20°48.8'	20°39.3'
E. Longitude	39°51.3'	39°51.3'	39°54.0'	39°40.5'	39°56.5'	39°53.8'	39°52.9'	39°47.5'
$^{206}Pb/^{204}Pb$	18.03	18.39	18.32	18.56	18.33	18.21	18.23	18.16
$^{206}Pb/^{204}Pb(i)$	18.03	17.85	18.31	18.47	18.28	18.13	18.18	18.14
$^{207}Pb/^{204}Pb$	15.50	15.51	15.51	15.54	15.58	15.50	15.49	15.57
$^{208}Pb/^{204}Pb$	37.61	38.02	37.97	38.27	38.48	37.88	37.88	38.02
$^{87}Sr/^{86}Sr$	.70305±3	.70386±3	.72886±4	.70320±2	.70602±2	.70376±1	.70317±1	.70361±2
$^{87}Sr/^{86}Sr(i)$	.70297	.70350	.70250	.70313	.70580	.70367	.70311	.70350
$^{143}Nd/^{144}Nd$		.51295±1	.51292±1	.51292±1	.51286±2		.51298±2	.51285±2
ENd		6.2	5.7	5.7	4.4		6.7	4.1
U	0.19	9.44	0.81	0.49	0.76	0.18	0.29	0.08
Th	0.61	28.54	2.97	1.54	3.02	0.61	1.14	0.31
Pb	22.85	5.10	22.38	1.53	4.58	0.64	1.69	1.43
$^{238}U/^{204}Pb$	0.5	116.8	2.3	20.1	10.5	17.1	10.6	3.5
$^{232}Th/^{238}U$	3.4	3.1	3.8	3.3	4.1	3.3	4.1	4.0
Rb	30	62	130	30	55	40	20	<10
Sr	489	215	6.1	527	312	553	435	185
Nd		39.50	59.83	25.01	4.60		26.44	7.56
Sm		9.11	12.97	5.48	10.40		6.59	2.29
$^{147}Sm/^{144}Nd$		.139	.131	.132	.182		.151	.183
$Pb/SrX10^3$	4.7			2.9	14.7	1.1	3.9	7.7
delta-8/4			21	31		33	27	

	Damm complex dikes			Sita Formation lavas				
Sample No.	165575	175825	165791	165714	165766	165767	165768	165772
Rock type	Basalt	Trachyte	Diabase (basalt)	Perlite (rhyolite)	Trachyte	A.basalt	Basalt	Basalt
N. Latitude	20°47.7'	20°54.6'	20°57.1'	20°44.5'	20°57.9'	20°57.5'	20°58.1'	20°58.4'
E. Longitude	39°51.3'	39°42.0'	39°41.4'	39°38.0'	39°36.7'	39°37.2'	39°37.0'	39°38.3'
$^{206}Pb/^{204}Pb$	18.04	18.66	18.17	18.32	18.97	18.25	18.21	18.40
$^{206}Pb/^{204}Pb(i)$	18.03	18.56	18.15	18.28	18.83	18.19	18.17	18.27
$^{207}Pb/^{204}Pb$	15.52	15.53	15.51	15.52	15.56	15.51	15.54	15.53
$^{208}Pb/^{204}Pb$	37.74	38.27	37.82	37.71	38.72	37.92	38.10	38.15
$^{87}Sr/^{86}Sr$	.70303±2	.70397±3	.70356±2	.71661±3	.70346±2	.70340±3	.70333±2	.70318±2
$^{87}Sr/^{86}Sr(i)$	.70297	.70319	.70350	.70060	.70322	.70337	.70327	.70311
$^{143}Nd/^{144}Nd$	.51295±2	.51293±1		.51284±1		.51297±1	.51299±1	.51294±2
ENd	6.2	5.7		4.0		6.5	6.9	6.1
U	0.17	2.75	0.15	2.74	2.98	0.31	0.44	0.31
Th	0.60	9.39	0.45	7.16	8.35	0.96	1.38	0.96
Pb	4.77	7.93	2.22	17.83	6.64	1.79	3.10	0.68
$^{238}U/^{204}Pb$	2.3	22.0	4.2	9.6	28.8	11.1	8.9	29.0
$^{232}Th/^{238}U$	3.6	3.5	3.1	2.7	2.9	3.2	3.2	3.2
Rb	26	94	21	127	108	10	31	27
Sr	521	162	428	9.8	562	440	601	513
Nd	24.71	39.89		60.43		21.53	24.00	22.12
Sm	6.05	8.10		13.93		5.64	5.59	5.13
$^{147}Sm/^{144}Nd$	.148	.123		.139		.158	.141	.140
$Pb/SrX10^3$	9.2		5.2			4.1	5.2	1.3
delta-8/4		20			33	30		

Table 1.—Pb, Sr, and Nd isotopic compositions (continued)

	Sita Formation lavas	Proterozoic Basement					
Sample No.	175826	165735	165672	165556	165611	165542	165008
Rock type	Trachybasalt	Granite-gneiss	Mu-Qtz schist	Granite-gneiss	Granite-gneiss	Granite gneiss	Ky-Mu quartzite
N. Latitude	20°54.6'	20°58.3'	20°45.8'	20°47.1'	20°46.2'	20°44.1'	20°46.2'
E. Longitude	39°42.0'	39°59.0'	39°45.2'	39°52.7'	39°55.9'	39°54.7'	39°47.6'
$^{206}Pb/^{204}Pb$	18.86	18.01	18.72	18.39	18.14	18.84	18.89
$^{206}Pb/^{204}Pb(i)$	18.73	17.98	18.63	18.35	18.12	18.80	18.83
$^{207}Pb/^{204}Pb$	15.54	15.51	15.58	15.53	15.52	15.56	15.57
$^{208}Pb/^{204}Pb$	38.58	37.76	37.76	38.35	38.22	37.77	37.51
$^{87}Sr/^{86}Sr$	.70329±2	.70863±3	.71884±2	.71146±2	.70660±4	.71733±3	.71958±3
$^{87}Sr/^{86}Sr(i)$	.70319						
$^{143}Nd/^{144}Nd$	.51295±1	.51244±2	.51257±2	.51257±2	.51247±2	.51254±1	.51239±3
ENd	6.3	-3.9	-1.3	-1.3	-3.3	-1.9	-4.8
U	.54	1.43	1.24	1.68	0.88	3.17	0.87
Th	1.83	5.54	3.73	10.94	9.71	7.42	0.85
Pb	1.28	16.39	3.91	14.42	14.17	22.87	4.08
$^{238}U/^{204}Pb$	27.1	5.5	20.1	7.4	3.9	8.8	13.4
$^{232}Th/^{238}U$	3.5	4.0	3.1	6.7	11.3	2.4	1.0
Rb	42						
Sr	521	476	65.4	203	602	37.3	30.2
Nd	20.87	29.30	12.28	63.7	26.40	15.76	6.54
Sm	4.48	4.46	2.35	11.38	3.60	2.83	1.03
$^{147}Sm/^{144}Nd$	.130	.092	.116	.108	.082	.108	.095
$Pb/SrX10^3$	2.4						
delta-8/4	31						

Pb isotopic compositions have variable $^{206}Pb/^{204}Pb$ ratios and plot in, and slightly above, the MORB field, consistent with depleted asthenospheric sources and the presence of small amounts of old continental Pb in some samples (fig. 4). Alkalic and subalkalic (mostly tholeiitic) samples plot on the same data trend, but the subalkalic rocks show lower and less variable $^{206}Pb/^{204}Pb$ than the alkalic rocks. The subalkalic rocks alone appear to be enriched with an old crustal Pb component, as shown by high $^{207}Pb/^{204}Pb$ and $^{208}Pb/^{204}Pb$. This component is similar to Pb in Indian Ocean sediments and in exotic ancient continental rocks within the Arabian-Nubian Shield (ANS) (Stacey and Stoeser, 1983); it is unlike Pb in the Late Proterozoic basement rocks in the Al Lith area. The alkalic volcanic and hypabyssal rocks from Al Lith extend the data trend to higher $^{206}Pb/^{204}Pb$. Isotopic data for Late Proterozoic Al Lith basement rocks overlap those for the Tertiary samples and plot (in some cases) below the MORB field, indicating isotopic evolution with low Th/U. Low Th/U ratios in continental crustal rocks are unusual, but have been recognized in the arc-type rocks of the Wadi Tarib batholith in the southern Arabian Shield (Stacey and Stoeser, 1983). Most of the basement samples do not plot above the MORB field, as in the case for many of the subalkaline Tertiary rocks; therefore, contamination by Pb from these upper crustal rocks is precluded. Adjustment of the MORB envelope for 30 Ma, the average age of Al Lith magmas, results in a slight shift of the present-day MORB field to lower $^{206}Pb/^{204}Pb$ ratios with no significant change in $^{207}Pb/^{204}Pb$ ratios, and does not affect the interpretation of the data.

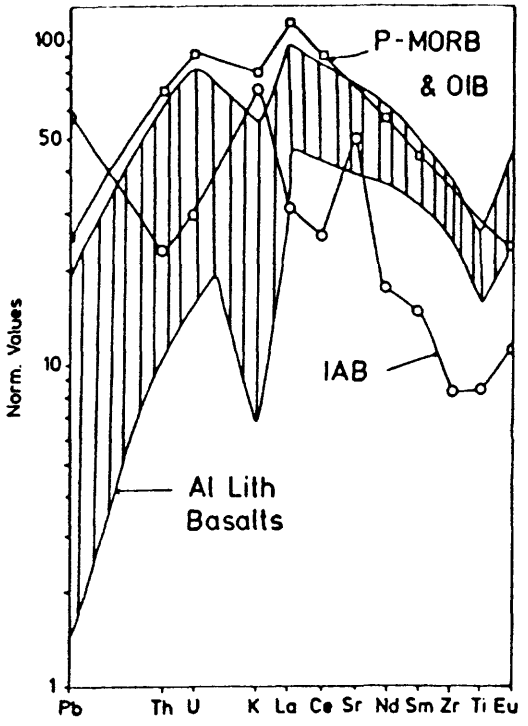

Figure 2.--Comparison of extended LREE distribution paterns in enriched Al Lith basalts, plume-type mid-ocean ridge basalts (P-MORB) and ocean island basalts (OIB), and LREE-enriched island arc basalts (IAB). Normalizing values, sequence of elements an abscissa and element patterns for P-MORB and OIB and IAB from Sun (1980). LREE, K, Zr and Ti concentrations from Pallister (1987).

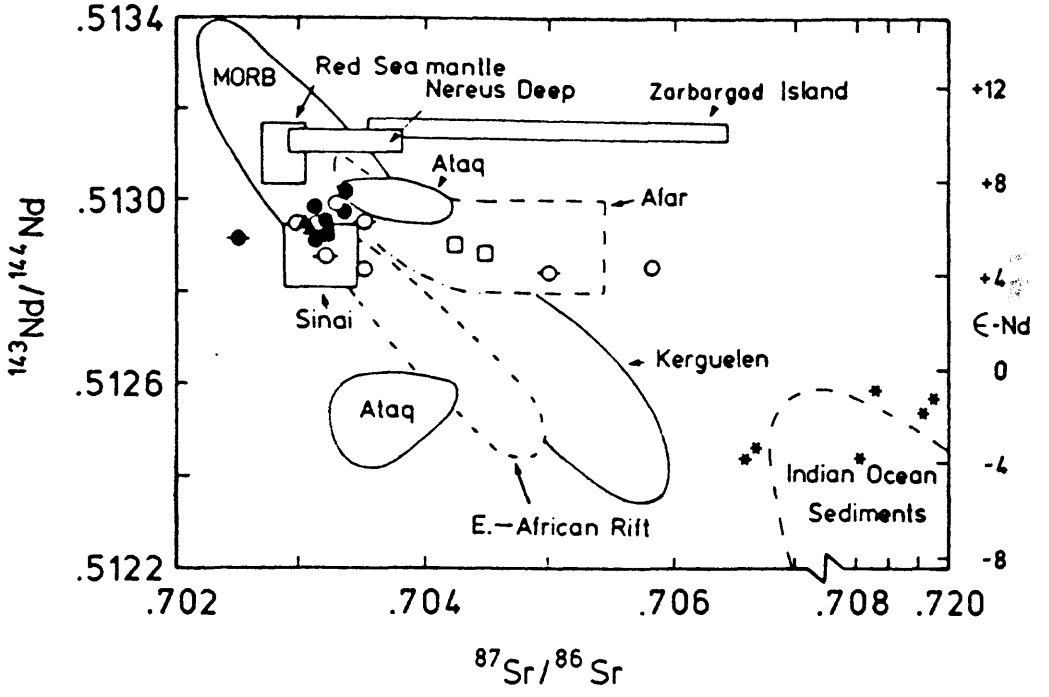

Figure 3.—$^{87}Sr/^{86}Sr$ vs. $^{143}Nd/^{144}Nd$ isotopic compositions in Al Lith volcanics. Sources: MORB, Kerguelen, Indian Ocean sediments (White, 1985); Ataq (Menzies and Murthy, 1980); Afar (Betton and Civetta, 1984); East African Rift (Bell and Blenkinsop, 1987; Cohen and others, 1984); Nereus Deep and Brothers Islands, Petrini, 1987); Red Sea mantle (Betton and Civetta, 1983; Stein and others, 1987). Symbols: alkalic rocks (solid symbols); tholeiitic rocks (open symbols); felsic rocks (symbols with bars); Sita formation and Damm dike complex (circles); Gumayqah dikes (squares); Miocene and Pliocene flood basalts (triangles); Al Lith upper crustal basement (asterisks).

CRUSTAL CONTAMINATION

We believe that primary (mantle-derived) isotopic ratios are apparent in the Al Lith data, but, before discussing the implications of these ratios, it is necessary to evaluate the degree to which crustal contamination has obscured these primary ratios. In the following two sections we deal primarily with anomalous radiogenic data from several of the subalkaline rocks that suggest contamination. Magma contamination is a common process in continental volcanics and studies have shown that in regions of thick continental crust, contamination occurs preferentially in the lower crust during underplating of dense mafic magmas (for example, Ewart and others, 1980; Cox, 1980; Hanson, 1981; Dickin, 1981; Herzberg and others, 1983; Carlson, 1984) and commonly results in the production of large volumes of fractionated silicic rocks (for example, Moorbath and Welke, 1969; Moorbath and Thompson, 1980). We conclude from the evolved nature of many Al Lith basalts and the lack of mantle xenoliths that some Al Lith magmas resided in the crust before eruption and were consequently prone to contamination.

$^{87}Sr/^{86}Sr$ isotopic compositions in some of the basalts are anomalously radiogenic (table 1, fig. 3), possibly due to magmatic assimilation of continental crust and/or to ground or seawater contamination during low-grade metamorphism. These possibilities can be investigated by plotting Sr isotopic compositions versus Pb/Sr ratios (fig. 5a). Sr isotopic compositions are high in evolved crustal rocks and groundwater or seawater, but, the Pb/Sr ratio of the crust can greatly exceed that in water. Mantle-derived melts have both low Sr isotopic compositions and Pb/Sr ratios such that mixing with crust shows as a positive linear trend in figure 5a. Most of the Al Lith basalts (tholeiitic and alkaline) fall on a well-developed positive data trend with a modest variation in Sr isotopic ratios (fig. 5a, inset) suggesting a minor crustal component even in the basalts with relatively low $^{87}Sr/^{86}Sr$. Tholeiites plotting to the right of the mantle array in the Nd-Sr isotopic correlation diagram (fig. 3) lie closest to crustal rocks, in agreement with crustal contamination. These basalts also have distinctly lower Sr/Nd ratios than samples that plot in the MORB-field, favoring a crustal component. Two of the three basalts with very radiogenic Sr belong to the Gumayqah complex and were collected from wide dikes (10-100m), a setting that apparently favors crustal contamination (Patchett, 1980). These samples contain excess radiogenic argon, consistent with crustal contamination (Pallister, 1987).

ϵ -Nd values plotted versus Pb/Sr ratios in tholeiitic and alkalic basalts show a crude negatively-correlated mixing trend between crust and mantle-derived magma with low Pb/Sr and high ϵ -Nd values (fig. 5b). Five of the tholeiites plot closer to crustal compositions, suggesting that their low ϵ -Nd values are produced by crustal contamination.

Covariation of ϵ -Nd values and $^{206}Pb/^{204}Pb$ ratios in mafic and felsic samples are shown in figure 6. Samples with tholeiitic chemistry generally have lower $^{206}Pb/^{204}Pb$ isotopic ratios and in many cases lower ϵ -Nd values than alkali basalts.

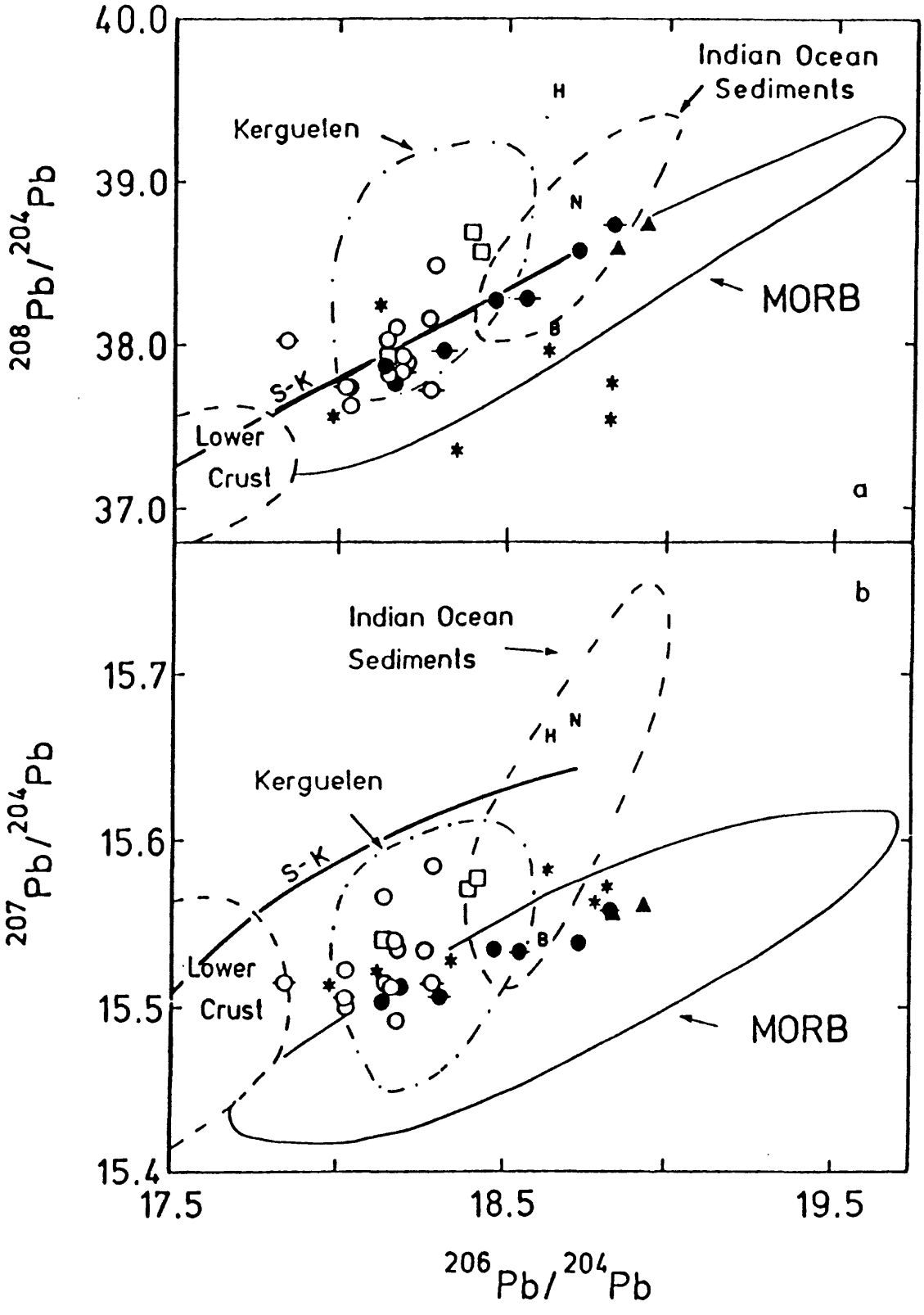

Figure 4.--Pb isotopic compositions in Al Lith rocks. Fields for lower crust are based on data from Precambrian rocks of the west-central ANS (see text; Stacey and Stoeser, 1983). Other data fields from White (1985). Stars represent selected Pan-African arc rocks from Stacey and Stoeser (1983). Additional data from Delevaux and others (1967): B = Red Sea brine, H = Hailan galena from Yemen, N = Wadi Nuji galena from Oman. Symbols as in figure 3.

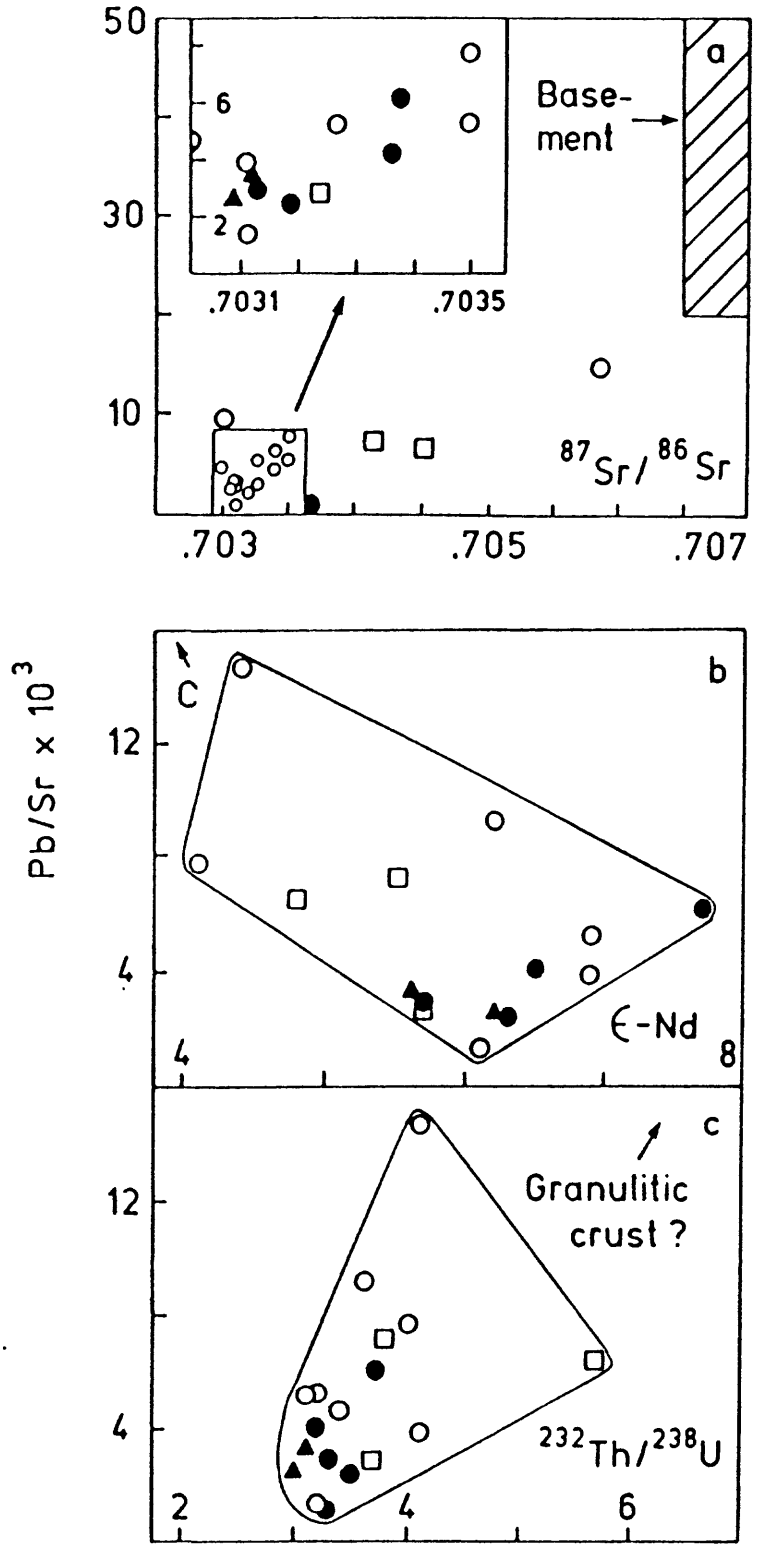

Figure 5.--Variations of Pb/Sr with $^{87}Sr/^{86}Sr$, ϵ-Nd and $^{232}Th/^{238}U$ in Al Lith volcanics. Only basaltic rocks are plotted. Symbols as in figure 3, except continental crust indicated by capital letter C.

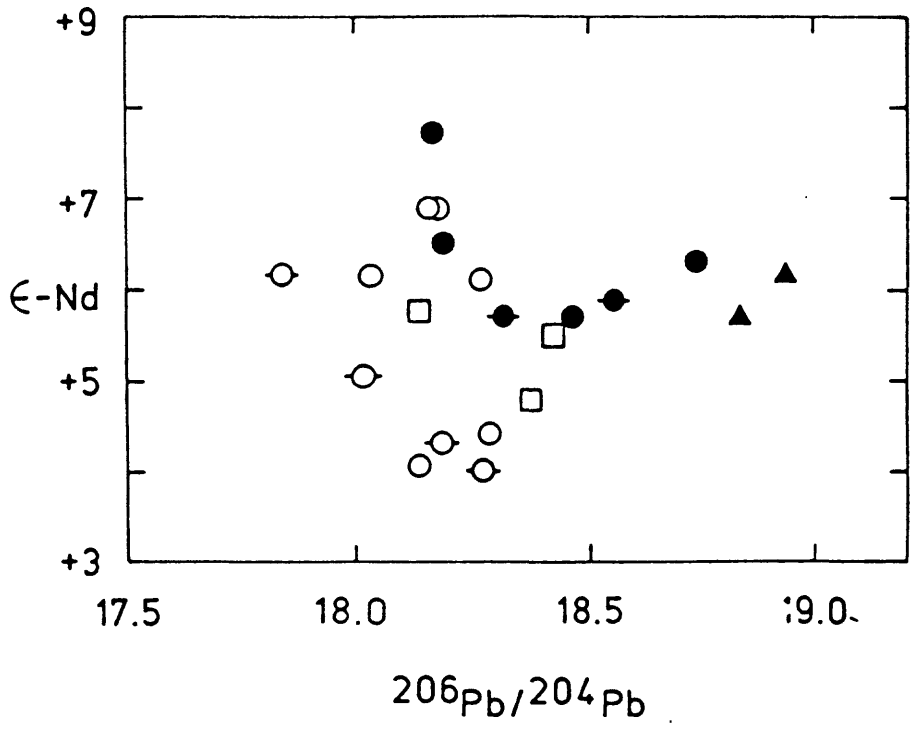

Figure 6.—$^{206}Pb/^{204}Pb$ ratios versus ϵ -Nd values in Al Lith volcanics. Symbols as in figure 3.

Because addition of only small amounts of continental material result in a crustal Pb signature in basaltic magmas, the low $^{206}Pb/^{204}Pb$ ratios in some (but not all) tholeiites likely reflect the presence of a crustal component with relatively unradiogenic Pb and Nd. This contaminant may be lower crustal granulite; however, some upper crustal basement samples also have relatively unradiogenic $^{206}Pb/^{204}Pb$ isotopic ratios (fig. 4).

Possible granulitic contamination can be investigated by the Th/U versus Pb/Sr relationship in figure 5c. Granulites are generally characterized by high Th/U due to removal of U during metamorphism. The data points fan out towards higher Th/U ratios with increasing Pb/Sr ratios, generally in agreement with a granulitic mixing member. However, the large scatter in the data suggests substantial heterogeneity in the Th/U of the crust and probable mobility of U during weathering. Partial melting is able to fractionate Th/U ratios, but, the effect is small compared to the variation seen in Al Lith basalts.

Figure 4 shows calculated fields for possible lower-crustal compositions based on the initial isotopic compositions in upper-crustal Pan-African arc rocks of the southwestern Arabian Shield (Stacey and Stoeser, 1983). Many of the tholeiites have more radiogenic $^{207}Pb/^{204}Pb$ and $^{208}Pb/^{204}Pb$ ratios than MORB, requiring a

more-ancient component of continental Pb than seen in our Pan-African basement samples and inferred lower crust. An ancient Pb component has been identified in rocks from areas surrounding the Pan-African oceanic assemblage of the central ANS (fig. 1) and is considered to reflect detritus from Archean basement (Stacey and Stoeser, 1983; Stacey and Agar, 1985). Recent discovery of old detrital and xenocrystic zircons in regions of the ANS with Pan-African oceanic basement indicate that ancient sediments may have a wide distribution in the ANS (Kroner and others, 1987; Pallister and others, 1987). Assimilation of only a few percent of such a component (which could also be preserved in the lower crust) may explain the anomalous Pb-isotopic compositions in some tholeiitic samples.

It is important to stress that most of the Al Lith basalts show little evidence of crustal contamination. Even among the subalkaline rocks, there are several that appear uncontaminated. For example, tholeiite 175780 ($^{206}Pb/^{204}Pb$ = 18.18) has oceanic Ce/Pb (see Hofmann and others, 1986 for comparison), low Pb/Sr, and high ϵ-Nd, and tholeiite 165772 has one of the lowest combined Pb/Sr and $^{232}Th/^{238}U$ ratios (fig. 5c). We also note that the Al Lith felsic volcanics are isotopically similar to the basaltic rocks (figs. 3-5), consequently, their evolved compositions cannot be attributed to large-scale assimilation of crustal rocks. The Al Lith basement data shows that Pb isotopic ratios are not adequate discriminants for crustal contamination, but there is no systematic shift of the felsic samples to higher Sr and lower Nd isotopic ratios. Origin as products of fractional crystallization of the basaltic rocks, or as anatectic melts of mafic precursors emplaced in the lower crust are viable alternatives.

Dickinson and others (1969) noted that, despite abundant silicic volcanics at several Pliocene-Miocene volcanic centers in southern Yemen, Rb and Sr isotopic data not only precluded upper crustal contamination, but also gave an apparent Rb-Sr age 20 to 30 m.y. greater than the age of eruption. They attributed this age to local mantle melting and fractionation during production of the preceeding Yemen Trap Series. Twenty years later, we find that our isotopic data also records Tertiary mantle enrichment processes that preceeded eruption, with only limited evidence of crustal contamination.

CRUSTAL CONTAMINATION OR DUPAL MANTLE SOURCES?

It has been proposed that anomalous Pb in young Red Sea basalts indicate Dupal source characteristics (Altherr and others, 1987). Dupal mantle sources can be explained by ancient (>3 Ga; Hart, 1984) contamination of a MORB reservoir with sediments (Dupre and Allegre, 1983) as seen in basalts belonging to the Kerguelen group (White, 1985). A robust identification criterion is the high Δ-8/4 (the deviation of the measured $^{208}Pb/^{204}Pb$ ratio from a northern hemisphere basalt regression line; Hart, 1984) and accompanying radiogenic Sr isotopic compositions. It is obvious that true Dupal mantle sources are difficult to distinguish from isotopic

signatures produced by contamination of a MORB-like magma with an ancient crustal component during magma transport through continental crust.

The similarity of Nd and Sr isotopic compositions in Al Lith basalts with those in young volcanics from the Red Sea region (Cohen and others, 1980; Coleman and others, 1983; Betton and Civetta, 1984; Barberi and others, 1987; Petrini, 1987) suggests similar sources. Interpretation of our data as the result of magma generation from "normal" oceanic mantle sources (that have recently been enriched with incompatible-elements - see below) and subsequent crustal contamination (detectable in some of the magmas) are in conflict with the interpretation of Red Sea basalt data as indicating Dupal sources.

The presence of Dupal mantle sources should also be apparent in Pan-African igneous rocks from Red Sea region, because of the inferred ancient origin of the anomaly (Hart, 1984), although, some rocks in the Pan-African might be allochthonous and unrelated to the mantle sources for Red Sea rift basalts. Pb isotopic compositions, measured on a large number of Pan-African samples from the central part of the ANS, are oceanic (Stacey and Stoeser, 1983). Initial Δ-8/4 values that we calculate for these rocks range from -3 to -22 and are clearly anti-Dupal (Δ-8/4 values were determined by calculating a northern hemisphere basalt reference line for the age of the samples using a $^{238}U/^{204}Pb$ ratio of 8 and a Th/U ratio of 2.5 in the MORB-reservoir; Allegre and Condomines, 1982). Alkalic rift-related volcanics from Al Lith have values between +17 and +33 and are not particularly high. For comparison, a basalt from the Juan de Fuca ridge, a region with distinct anti-Dupal characteristics (Hart, 1984), has a Δ-8/4 value of +27 (sample VG 44, White and others, 1987).

Another important characteristic of Dupal mantle sources is coherent evolution with high time-integrated Rb/Sr, Th/U and $^{234}U/^{204}Pb$ ratios (Dupre and Allegre, 1983), thus, radiogenic Sr should be accompanied by Pb isotopic compositions plotting above the MORB-envelope. Available Sr isotopic compositions in young basalts from the Red Sea region are not particularly radiogenic, but are MORB-like (Coleman and others, 1983; Barberi and Chivetta, 1983; Altherr and others, 1987) and do not show a correlation with Pb isotopic compositions (Altherr and others, 1987). We conclude from these observations that evidence for ancient continental Pb in some Red Sea rift basalts probably reflects true crustal contamination, rather than mantle characteristics.

Anomalous Pb in tholeiitic Al Lith volcanics is best explained by crustal contamination involving an ancient sedimentary component. A source for old continental Pb can be seen in the occurrences of exotic ancient continental crust (sediments or crustal fragments) within the dominantly oceanic ANS (Stacey and Agar, 1985; Kröner and others, 1987). The fact that crustal signatures are best developed in rock types and isotopic systems most prone to record crustal contamination supports our conclusion for absence of Dupal mantle sources.

MANTLE SOURCES FOR AL LITH MAGMAS

The relatively simple geologic history of the Arabian-Nubian Shield (ANS) (formation by accretion of oceanic arcs and exotic continental fragments during the Late Proterozoic, then unaffected by tectonism and magmatism until Tertiary Red Sea rifting and volcanism) allows reasonable, but model-dependent, inferences to be drawn about the relative roles and evolution of underlying lithospheric and asthenospheric mantle source regions. We assume that lithospheric mantle was generated during Late Proterozoic oceanic-arc accretion of the ANS, and that it remained attached to the ANS crust at least until Red Sea rift activity commenced.

Isotopic Compositions

The lithospheric mantle of the central ANS (the Red Sea region) was presumably formed by accretion of the underpinnings of oceanic island arcs during the Late Proterozoic Pan-African orogeny. Initial ϵ-Nd values of up to +8.9 (Bokhari and Kramers, 1981; Duyverman and others, 1982; Claesson and others, 1984; Stein and others, 1987; this study) in combination with oceanic Pb in Pan-African rocks of island arc origin (Stacey and Stoeser, 1983) indicate derivation from MORB-like sources. Subduction of oceanic crust and accretion of at least six microplates were followed by crustal consolidation of the ANS between about 600 and 700 Ma to produce 40 km-thick continental crust (Stoeser and Camp, 1985; Pallister and others, 1987). There is little evidence in the extensive Paleozoic and Mesozoic stratigraphic record of Arabia for significant tectonism or magmatism in the central ANS; we assume that after consolidation, the sub-ANS mantle was isolated from asthenospheric convection until the onset of Tertiary rift magmatism. However, sometime after consolidation, and presumably during early rifting, the subcontinental mantle was locally enriched in incompatible elements (Thornber and Pallister, 1985; Henjes-Kunst, 1987; Brueckner and others, 1987; Stein and others, 1987).

The identification of crustally contaminated samples and the resulting data trends allow us to estimate primary source characteristics. Sr and Nd isotopic variations and Pb/Sr ratios, which we interpret as mixing trends between crustal contaminants and mantle-derived magma (figs. 5a and b), suggest a moderate variation in primary $^{87}Sr/^{86}Sr$ isotopic compositions from about 0.7030 to 0.7033, accompanied by a range in ϵ-Nd values from +6 to about +8. These estimates are based on the isotopic compositions in samples that plot farthest from crustal compositions in figure 5 and that appear to have been least contaminated (such as the alkali basalts and some tholeiites).

Determination of primary Pb isotopic characteristics is more difficult because of the large effects of crustal Pb on mantle-derived magmas. Alkali basalts that we consider less susceptible to contamination than tholeiites (due to their higher Pb concentrations) are similar to MORB. These data plot farthest from crustal

compositions on the mixing trends in fig. 5 and, unlike most of the tholeiites, we consider them as relatively reliable indicators of primary source characteristics. Because Nd and Sr isotopic compositions in alkali basalts and tholeiites indicate common sources, we believe that primary isotopic compositions in the tholeiites were similar to those in the alkali basalts. This conclusion assumes coherent fractionation of parent/daughter element ratios during chemical processes in the sources of both alkalic and tholeiitic basalts. We conclude that the sources of Al Lith tholeiites also have MORB-like Pb and moderately radiogenic $^{206}Pb/^{204}Pb$ isotopic ratios (ranging from 18.2 to 19.0) as seen in the alkalic rocks. It is intriguing that the alkali basalts do not show evidence of preferential tapping of isotopically-enriched low-melting anomalies, as is the case for alkalic seamount basalts. This may reflect a difference in residence time of incompatible-element enriched source regions in the two settings; insufficient time passed between incompatible-element enrichment of Al Lith sources and magma extraction for the isotopic ratios of Pb, Sr, and Nd to respond. The apparent isotopic similarity of tholeiites and alkali basalts, as well as similar incompatible-element (especially LREE) enrichment of both rock types (Pallister, 1987) suggests decoupling of major and trace elements, consistent with a CO_2-H_2O-fluid based enrichment process.

The inferred primary isotopic compositions of Al Lith volcanics indicate sources that had evolved with variable parent/daughter element ratios and that are somewhat less depleted than modern asthenosphere in the Red Sea region (fig. 3) and also less depleted than those for some Pan-African oceanic rocks (for example, Bokhari and Kramers, 1981). The degree of source heterogeneity is nevertheless small compared to that in Tertiary basalts from southwestern Arabia at Ataq (Menzies and Murthy, 1980) and from the East African Rift (Bell and Blenkinsop, 1987; fig. 3).

Isotopic similarity in the 30 Ma old Sita volcanics and 20 Ma Gumayqah dikes suggests no significant changes in the composition of the basalt sources below this region with time. In addition, Pliocene and Late Miocene alkali basalts from Al Lith apparently tapped the same reservoir as the Eocene to early Miocene volcanics. However, there was a significant shift to more depleted sources for young (<5 Ma) basalts at the Red Sea axis. These relations may be explained by coupling of the extended crustal margin with lithospheric mantle sources during rifting (see "Magma Generation and Mantle Evolution", this report).

TRACE ELEMENTS

$^{147}Sm/^{144}Nd$ ratios of 0.197 and 0.183 for two primitive ($\approx$10% MgO) tholeiites and 0.182 for one evolved ($\sim$5% MgO) tholeiite indicate flat to slightly LREE-enriched distribution patterns. A complete REE analysis of one of these samples yielded a flat REE pattern at 10-15 X chondritic abundance (Pallister, 1987). The degree of LREE enrichment in the high-Mg basalts is considered to

represent an upper limit for LREE enrichment of their sources because partial-melting and fractionation processes result in melts with higher LREE abundances than those in parental material.

In contrast, most Al Lith tholeiites and alkali basalts are uniformly LREE-enriched ($^{147}Sm/^{144}Nd < < 0.197$; see also Pallister, 1987) but few show significant Eu anomalies. The predominant LREE-enriched character of Al Lith basalts, in combination with high (radiogenically unsupported) $^{143}Nd/^{144}Nd$, indicates recent LREE enrichment of mantle sources. A similarity in HREE abundance levels for basalts with and without LREE enrichment (including samples with similar MgO contents), and the relatively high HREE contents ($\approx$10 X chondrite, Pallister, 1987) of all the basalts, indicates a lack of garnet in the mantle residue and favors origin of parent magmas for both types of basalts from the spinel-lherzolite facies of a mantle source region that was heterogeneous with respect to incompatible-element enrichment. Last equilibration of lherzolites in the spinel-lherzolite facies at Zarbagad Island (Bonatti and others, 1986) and the presence of garnet only as a reaction phase in xenoliths from Arabian harrat basalts (Thornber, 1988) is consistent with this interpretation.

REE and incompatible-element patterns (fig. 2 and Pallister, 1987) are subparallel to LREE-enriched MORB and OIB, indicating similar incompatible trace-element inventories of their sources. $^{232}Th/^{238}U$ ratios in the least-contaminated Al Lith basalts range between 3 and 3.5 and are high compared to the ratios in basalts from subduction zones (Tatsumoto, 1978; Allegre and Condomines, 1982). The evidence for "normal" oceanic mantle sources in Al Lith volcanics is somewhat surprising in the context of repeated subduction and arc-accretion during formation of the ANS.

The central region of the ANS is composed mainly of immature oceanic arc rocks. Given lithospheric sources for the Al Lith rocks, the lithospheric mantle below the central ANS must have remained oceanic (depleted) in character, despite its accretionary history and implied sediment "ingestion" from paleo-subduction zones. Ce/Pb ratios in tholeiite and hawaiite (samples 175780, 165561, and 165006, which show minimal crustal contamination and for which Ce concentrations are available) vary from 25 to 28, and lie in the range of oceanic basalts (Hofmann and others, 1986). Trace-element enrichment of the proto-Red Sea lithospheric mantle apparently began in some areas during the Late Proterozoic (Stein and others, 1987; Henjes-Kunst, 1987), but in the Al Lith data, we find evidence only for relatively recent enrichment; enrichment that must have occurred by a process that did not fractionate Ce/Pb, as assumed, for example, in melt metasomatism (Hofmann and others, 1986; and references therein).

MAGMA GENERATION AND MANTLE EVOLUTION

Contemporaneous extrusion of isotopically similar tholeiites and alkali basalts indicates similar sub-continental mantle exists over a large depth interval below the central Red Sea rift. In contrast, stratification of enriched and depleted basalt sources is inferred at Ataq (Menzies and Murthy, 1980), the East African Rift (Bell and Blenkinsop, 1987), and the Rio Grande Rift (for example, Perry and others, 1987). Pb isotopic compositions in Al Lith volcanics are moderately radiogenic to MORB-like, and Nd and Sr isotopes are slightly less depleted than young Red Sea basalt (Betton and Civetta, 1983) and MORB-type mantle below parts of the Sinai (Stein and others, 1987, fig. 3). Our data indicate that Al Lith volcanism tapped similar mantle sources during an extended period of rift-related magmatism. There is no clear indication for changing proportions of enriched lithospheric mantle to asthenospheric mantle below the rifted margin. However, younger basalts from the Red Sea axis show more depleted sources than Tertiary Al Lith volcanics, indicating a decreasing influence of enriched lithosphere. The lithosphere was displaced by an upwelling asthenospheric diapir that eventually reached the surface at the young (< 5 Ma) spreading axis of the Red Sea.

These observations can be explained in the context of various rifting hypotheses proposed for the development of Red Sea and East African Rifts (Bonatti and Seyler, 1987; Mohr, 1987; Searle, 1970; Baker and Wohlenberg, 1971). These models propose a rapid rise of the asthenosphere to the base of the crust and consumption of the continental lithosphere by thermal convection (Spohn and Schubert, 1982). They are consequently "active" in the sense of calling for erosion of the base of the lithosphere and conversion of lithosphere to asthenosphere. However, as pointed out by Coleman (1984), the proto-Red Sea was a topographic low prior to and during the initial stages of rifting; assymetric uplift (preferentially of the eastern margin) took place in two stages during the Miocene and Pliocene (Kohn and Eyal, 1981; Schmidt and others, 1982). Consequently, we consider the rifting to be (in general) a passive process, driven by plate motions.

Isotopic and trace-element signatures in the rift-related rocks can be attributed to incompatible-element metasomatism of the lithospheric mantle, probably involving CO_2-H_2O-fluids, during early rifting, followed by preferential melting of metasomatised regions over a significant depth interval, then by the replacement of the lithosphere by depleted asthenosphere and production of MORB at the spreading axis during the final "oceanic" stage. This model is shown diagramatically in figure 7. Enriched asthenospheric mantle may have been present at depth in other regions of the Red Sea-East Africa rift system (to account for isotopically enriched volcanics in other areas), but we lack evidence of long-term enriched mantle sources in the Al Lith area. Norry and others (1980) also noted that incompatible-element enrichments are not reflected in isotopic ratios of lavas from the East African rift in Kenya, and called on a relatively recent fluid-based enrichment of mantle sources.

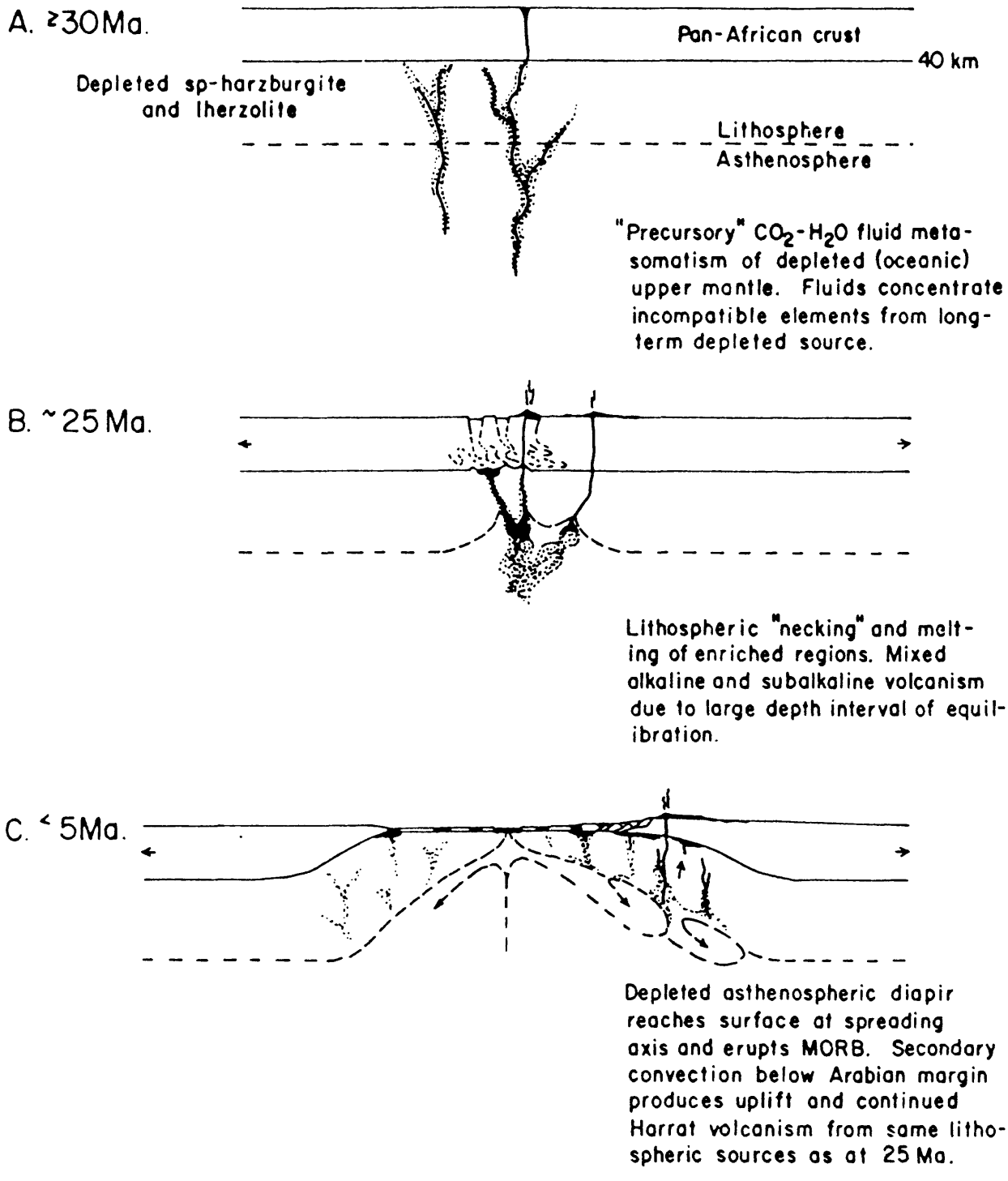

Figure 7.—Diagrammatic model for evolution of mantle source regions during Red Sea rifting. Crustal thickness approximate, from Mooney and others (1985).

Evidence for upwelling and fluid metasomatism below the ANS before and during early rifting is directly observed in uplifted sections that represent portions of the uppermost oceanic mantle in contact with lower continental crust at Zabargad Island (Bonatti and others, 1981, 1986; Bonatti and Seyler, 1987). There, spinel lherzolite with MORB-like Nd and Sr isotopic compositions was intruded, first by hydrous metasomatic solutions that formed amphibole peridotites, then by magmas that produced troctolites. The amphibole peridotites lie off the mantle array with low isotopic ratios of Nd and Sr; the troctolites have higher Sr isotopic ratios, attributed to the fossil imprint of Pan-African subduction on magmas intruded during Red Sea diapirism (Brueckner and others, 1987).

Magmas generated in the early stage of rifting may have locally accumulated in sills that underplated the lower crust. Limited crustal contamination and crystal fractionation probably resulted (Pallister, 1987). Magma ponding can be related to density contrasts between mafic magma and overlying felsic crust (Herzbert and others, 1983) and coupled with secondary convection (Steckler 1985), may have have triggered crustal uplift (as envisaged by McKenzie, 1984) in the Miocene and Pliocene.

ACKNOWLEDGMENTS

Discussions with Carl R. Thornber and his review of an early draft of this paper were important contributions, especially to our understanding of the xenolith data from the Red Sea region. We also benefitted from helpful reviews by John S. Stacey and David A. Sawyer. We thank Mitsunobu Tatsumoto for providing isotopic analytical facilities. This paper is based on work conducted by the authors under a work agreement with the Saudi Arabian Deputy Ministry for Mineral Resouurces.

DATA STORAGE

Data work and materials used in preparation of this report are archived as Data File USGS-DF-05-4 stored in the office of the U.S. Geological Survey Mission in Jeddah, Saudi Arabia.

No updated information was added to the Mineral Occurrence Documentation System (MODS) data bank and no new localities were established in connection with this work.

REFERENCES CITED

Altherr, R., Baumann, A., Henjes-Kunst, F., and Puchelt, H., 1987, Sr-Pb systematics of basalts from the axial trough of the Red Sea: Terra Cognita, v. 7 (Abstr.), p. 366.

Allegre, C.J., and Condomines, M., 1982, Basalt genesis and mantle structure studied through Th-isotopic geochemistry: Nature, v. 299, p. 21-24.

Baker, B.H., and Wohlenberg, J., 1971, Structure and evolution of the Kenya Rift Valley: Nature, v. 299, p. 538-542.

Barberi, F., Civetta, L., and Varet, J., 1980, Sr isotopic composition of Afar volcanics and its implications for mantle evolution: Earth and Planetary Science Letters, v. 50, p. 247-259.

Bell, K., and Blenkinsop, 1987, Nd and Sr isotopic compositions of East African carbonatites: Implications for mantle heterogeneity: Geology, v. 15, p. 99-102.

Betton, P.J., and Civetta, L., 1984, Strontium and neodymium isotopic evidence for the heterogeneous nature and development of the mantle beneath Afar (Ethopia): Earth and Planetary Science Letters, v. 71, p. 59-70.

Bokhari, F.Y., and Kramers, J.D., 1981, Island arc character and late Precambrian age of volcanics at Wadi Shwas, Hijaz, Saudi Arabia: Geochemical and Sr and Nd isotopic evidence: Earth and Planetary Science Letters, v. 54, p. 409-422.

Bonatti, E., Hamlyn, P., and Ottonello, G., 1981, Upper mantle beneath a young oceanic rift: Peridotites from the island of Zabargad (Red Sea): Geology, v. 9, p. 474-479.

Bonnatti, E., Ottonello, G., and Hamlyn, P., 1986, Peridotites from the island of Zabargad (St. John), Red Sea: Petrology and geochemistry: Journal of Geophysical Research, v. 91, p. 599-631.

Bonatti, E. and Seyler, M., 1987, Crustal underplating and evolution in the Red Sea rift: uplifted mantle/lower crust sections on Zabargad and Brothers Islands: Terra Cognita, v. 7, (Abstr.), p. 311.

Brueckner, H. K., Zindler, A., Seyler, M., and Bonatti, E., 1987, Zarbagad and the Pan-African and Miocene isotopic evolution of the sub-Red Sea mantle and crust: Geological Society of America Abstracts and Programs, v. 19, p. 603.

Carlson, R., 1984, Isotopic constraints on Columbia River flood basalt genesis and the nature of the subcontinental mantle: Geochimica et Cosmochimica Acta, v. 48, p. 2357-2372.

Claesson, S., Pallister, J.S., Tatsumoto, M., 1984, Samarium-neodymium data on two late Proterozoic ophiolites of Saudi Arabia and implications for crustal and mantle evolution: Contribution to Mineralogy and Petrology, v. 85, p. 244-252.

Cohen, R.S., O'Nions, R.K., and Dawson, J.B., 1984, Isotope geochemistry of xenoliths from East Africa: implications for development of mantle reservoirs and their interaction: Earth and Planetary Science Letters, v. 68, p. 209-220.

Cohen, R.S., Evenson, N.M., Hamilton, P.J., and O'Nions, R.K., 1980, U-Pb, Sm-Nd and Rb-Sr systematics of mid-ocean ridge basalt glasses: Nature, v. 283, p. 149-152.

Coleman, R.G., 1984, The Red Sea: A small ocean basin formed by continental extension and sea-floor spreading in International Geological Congress, 27th, Moscow, Proceedings: Utrecht, The Netherlands, v. 23, p. 93-121.

Coleman, R.G., Gregory, R.T., and Brown, G.F., 1983, Cenozoic volcanic rocks of Sauid Arabia: U.S. Geological Survey Open-File Report 83-788, 82 p.

Cox, K.G., 1980, A model for flood basalt vulcanism: Journal of Petrology, v. 21, p. 629-650.

Delevaux, H.M., Doe, B.R., and Brown, G.F., 1967, Preliminary lead isotope investigations of brine from the Red Sea, galena from the Kingdom of Saudi Arabia, and galena from the United Arab Republic (Egypt): Earth and Planetary Science Letters, v. 3, no. 2, p. 139-144.

DePaolo, D.J., and Wasserburg, G.J., 1976, Inferences about magma sources and mantle structure from variations of $^{143}Nd/^{144}Nd$: Geophysical Research Letters, v. 3, p. 249-252.

Dickin, A.P., 1981, Isotope geochemistry of Tertiary igneous rocks from the Isle of Skye, NW Scotland: Journal of Petrology, v. 22, p. 155-189.

Dickenson, D. R., Dodson, M. H., and Gass, I. G., 1969, Correlation of initial $^{87}Sr/^{86}Sr$ with Rb/Sr in some late Tertiary volcanic rocks of south Arabia: Earth and Planetary Science Letters, v. 6, p. 84-90.

Dupre, B., and Allegre, C.J., 1983, Pb-Sr isotope variation in Indian Ocean basalts and mixing phenomena: Nature, v. 503, p. 142-146.

Duyverman, H.J., Harris, N.B.W., and Hawkesworth, C.J., 1982, Crustal accretion in the Pan African: Nd and Sr isotope evidence from the Arabian Shield: Earth and Planetary Science Leters, v. 59, p. 315-326.

Ewart, A., Baxter, K., and Ross, J.A., 1980, The petrology and petrogenesis of the Tertiary anorogenic mafic lavas of southern and central Queensland, Australia--possible implications for crustal thickening: Contributions to Mineralogy and Petrology. v. 75, p. 129-152.

Hanson, G.N., 1981, Geochemical constraints on the evolution of the early continental crust: Philosophical Transactions of the Royal Society of London, Ser. A, v. 301, p. 423-442.

Hart, S.R., 1984, A large-scale isotope anomaly in the southern hemisphere mantle: Nature, no. 309, p. 753-757.

Herzberg, C.T., Fyfe, W.S., and Carr, M.J., 1983, Density constraints on the formation of the continental Moho and crust: Contributions to Mineralogy and Petrology, v. 84, p. 1-5.

Hofmann, A.W., Jochum, K.P., Seufert, M., and White, W.M., 1986, Nb and Pb in oceanic basalts: New constraints on mantle evolution: Earth and Planetary Science Letters, v. 79, p. 33-45.

Kohn, B.P., and Eyal, M., 1981, History of uplift of the crystalline basement of the Sinai and its relation to opening of the Red Sea as revealed by fission track dating of apatites: Earth and Planetary Science Letters, v. 52, p. 129-141.

Krö ner, A., Reischmann, T., and Grieling, R., 1987, Pan-African crustal evolution in the Nubian segment of northeast Africa: Geological Association of Canada, Program with Abstracts v. 12, p. 65.

McKenzie, D., 1984, A possible mechanism for epeirogenic uplift: Nature, v. 307, p. 616-665.

Menzies, M., 1983, Mantle ultramafic xenoliths in alkaline magmas: evidence for mantle heterogeniety modified by magmatic activity, in Hawkensworth, J.C., and Norry, M. J., eds., Continental basalts and mantle xenoliths: Shiva Publishing Ltd., Cheshire, U.K., p. 92-110.

Menzies, M., and Murthy, V.R., 1980, Nd and Sr isotope geochemistry of hydrous mantle nodules and their host alkali basalts: Implications for local heterogeneities in metasomatically veined mantle: Earth and Planetary Science Letters, v. 46, p. 323-334.

Mohr, P., 1987, Structural style of continental rifting in Ethiopia: Reverse decollements: Transactions of the American Geophysical Union (EOS), v. 68, p. 728-730.

Mooney, W.D., Gettings, M.E., Blank, H.R., and Healy, J.H., 1985, Saudi Arabian seismic-refraction profile: A traveltime interpretation of crustal and upper mantle structure: Tectonophysics, v. 111, p. 173-246.

Moorbath, S., and Welke, H., 1969, Lead isotope studies on igneous rocks from the Isle of Skye, northwest Scotland, Earth and Planetary Science Letters, v. 5., 217-230.

Moorbath, S., and Thompson, R. N., 1980, Strontium isotope geochemistry and petrogenesis of the early Tertiary lava pile of the Isle of Skye, Scotland, and other basic rocks from the British Tertiary Province: an example of magma-crust interaction, Journal of Petrology, v. 21, p. 295-321.

Norry, M. J., Truckle, P. H., Lippard, S. J., Hawkesworth, C. J., Weaver, S. D., and Marriner, G. F., 1980, Isotopic and trace element evidence from lavas, bearing on mantle heterogeneity beneath Kenya: Philosophical Transactions of the Royal Society of London, A297, p. 259-271.

Pallister, J.S., Stacey, J.S., Fischer, L.B., and Premo, W.R., 1987, Arabian Shield ophiolites and late Proterozoic microplate accretion: Geology, v. 15, p. 320-323.

Pallister, J.S., 1987, Magmatic history of Red Sea rifting: Perspective from the central Saudi Arabian coastal plain: Geological Society of America Bulletin, v. 98, p. 400-417.

Patchett, P.J., 1980, Thermal effects of basalt on continental crust and crustal contamination of magmas: Nature, v. 382, p. 559-561.

Perry, F.V., and Baldridge, W.S., and DePaolo, D.J., 1987, Role of asthenosphere and lithosphere in the genesis of late Cenozoic basaltic rocks from the Rio Grande rift and adjacent regions of the southwestern United States: Journal of Geophysical Research, v. 92 (B9), p. 9193-9214.

Petrini, R., 1987, Nd-Sr isotopes on samples from the Brothers Island and Nereus Deep in the Red Sea: Terra Cognita, v. 7 (Abstr.), p. 396.

Schmidt, D.L., Hadley, D.G., and Brown, G.F., 1982, Middle Tertiary continental rift and evolution of the Red Sea in southwestern Saudi Arabia: U.S. Geological Survey Open-File Report 83-641, 56 p.

Searle, R.C., 1970, Evidence from gravity anomalies for thinning of the lithosphere beneath the Rift Valley in Kenya: Geophysical Journal of the Royal Astronomical Society, v. 21, p. 13-31.

Spohn, T., and Schubert, G., 1982, Convective thinning of the lithosphere: A mechanism for the initiation of continental rifting: Journal of Geophysical Research, v. 87, p. 4669-4681.

Stacey, J. S., and Agar, R. A., 1985, U-Pb isotopic evidence for the accretion of a continental microplate in the Zalm region of the Saudi Arabian Shield: Journal of the Geological Society of London, v. 142, p. 1189-1203.

Stacey, J.S., and Stoeser, D.B., 1983, Distribution of oceanic and continental leads in the Arabian Nubian Shield: Contributions to Mineralogy and Petrology, v. 84, p. 91-105.

Steckler. M.S., 1985, Uplift and extension at the Gulf of Suez - Indications of induced mantle convection: Nature, v. 317, p. 135-139

Stein, M., Hofmann, A.W., Goldstein, S.L., 1987, Lithospheric evolution of the northern Arabian Shield: Nd and Sr isotopic evidence from basalts, xenoliths and granites: Terra Cognita, v. 7 (Abstr.), p. 418.

Stoeser, D.B., and Camp, V.E., 1985, Pan-African microplate accretion of the Arabian Shield: Geological Society of America Bulletin, v. 96, p. 817-826.

Sun, S.S., 1980, Lead isotopic study of young volcanic rocks from mid-ocean ridges, ocean island and island arcs: Philosophical Transactions of the Royal Society of London, v. A-297, p. 409-455.

Tatsumoto, M., 1978, Isotopic compositions of lead in oceanic basalt and its implication to mantle evolution: Earth and Planetary Science Letters, v. 38, p. 63-87.

Thornber, C.R., and Pallister, J.S., 1985, Mantle xenoliths from northern Saudi Arabia: Transactions of the American Geophysical Union (EOS), v. 66, p. 393.

Thornber, C. R., 1988, Hutaymah pyroxenite xenoliths: Clues to the character of subcontinental mantle during early stages of Red Sea rifting: Geological Society of America Abstracts and Programs (in press).

White, W.M., 1985, Sources of oceanic basalts: Radiogenic isotope evidence: Geology, v. 13, p. 115-118.

White, W.M., Hofmann, A.W., and Puchelt, H., 1987, Isotope geochemistry of Pacific mid-ocean ridge basalt: Journal of Geophysical Research, v. 92, p. 4881-4893.